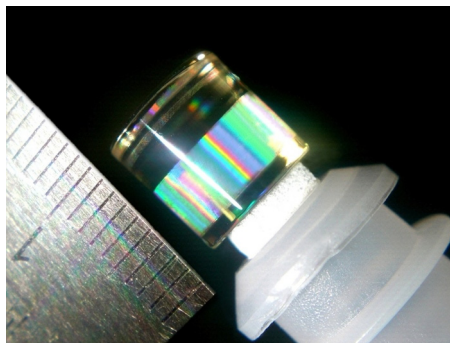# Cylindrical Grating Projection by Single-Shot Normal Exposure of a Radial Phase Mask

Volume 4, Number 4, August 2012

Svetlen Tonchev
Yves Jourlin
Stéphanie Reynaud
Olivier Parriaux

Cylindrical Grating Projection by Single-Shot Normal Exposure of a Radial Phase Mask

Svetlen Tonchev, [1] **Yves Jourlin,** [2] **Stéphanie Reynaud,** [2] **and Olivier Parriaux** [2]

[1] Institute of Solid State Physics, Bulgarian Academic of Sciences, 1784 Sofia, Bulgaria
[2] Université de Lyon, Laboratoire Hubert Curien, UMR CNRS 5516, 42000 Saint-Etienne, France

Abstract: A periodic grating is defined at the photoresist-coated wall of a circular cylinder with an integer number of particularly long grooves parallel to the generic lines by the holistic exposure of a radial phase mask to a normally incident collimated laser beam. The single-shot projected element corresponds to the inner grating of a high-resolution miniature shaft encoder.

Index Terms: Photolithography, phase masks, cylindrical gratings.

1. Introduction

The optics of cylindrical waves and beams is gaining interest with the development of axicons [1] and of beams of radial and azimuthal polarization distribution [2]. Whereas the shelf of planar optical elements for plane waves is very well provided due to the microstructuring potential borrowed from microelectronics, that for the processing of cylindrical waves is still to be completed; there is one element in particular that is missing: it is a cylindrical grating at the wall of a cylinder with an integer number of grooves parallel to its generic lines. Such a grating would naturally diffract a cylindrical wave produced, for instance, by a high aperture objective or a cone deflecting an azimuthally or radially polarized incident beam coaxial with the cylinder. In particular, when associated with a cone of 90° apex, it could be the core element in a new generation of high-resolution miniature shaft encoders [3], in biosensors, and potentially in the generation of new resonance effects in cylindrical resonators of an enlarged micro-gear type [4]. The reason why such an element with subwavelength features does not exist is that it has been impossible to fabricate so far with a perfect stitching between the first and last written line(s). The present paper describes and demonstrates a single exposure fabrication method for a uniform and stitchingless cylindrical grating comprising an integer number of lines by resorting to a phase-mask method that allows a standard planar radial grating pattern to be geometrically transformed and optically transferred into a cylindrical photoresist pattern at the circular wall of a cylinder. The planar radial grating pattern can be easily written with an integer number of lines having strictly constant period without stitching errors by means of the available tools of planar technologies such as a laser or electron beam generator and reactive ion etching. The reported cylindrical grating fabrication method is only an origination technique, after which an injection molding or embossing insert has to be configured to enable large volume manufacturing. The driving application is in rotary encoders [3]; therefore, the demonstrator will be configured accordingly.
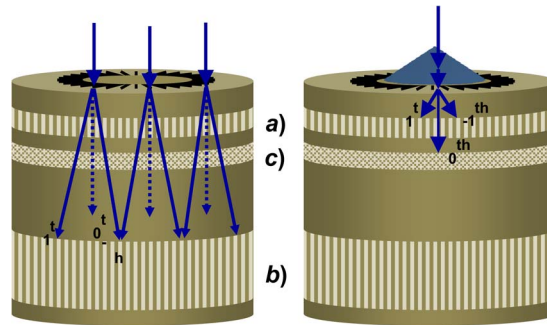
Fig. 1. Coaxial holistic exposure configuration for planar radial phase-mask projection onto the wall of a cylinder. (Left) Under normal incidence. (Right) Under a cylindrical wave by means of a cone as in [5].

2. The Interferogram Formation

The geometrical arrangement for creating a cylindrical grating at the wall of a cylinder with lines parallel to the cylinder axis is represented in perspective in Fig. 1(a). A collimated laser beam, parallel to the cylinder axis, having a circularly symmetrical polarization distribution (azimuthal or radial), impinges normally onto a phase mask made of radial lines and grooves defined in a ring-form area of internal and outer radii R_i and R_e. The ring is precisely centered on the cylinder axis, and the grating line prolongations all intersect the axis. The radial phase-mask grating is characterized by an angular period Λ_Φ equal to $2\pi/N$, where N is the integer number of periods; it diffracts in transmission the normally incident collimated beam in a number of orders that propagate with a zero radial k-vector component into the transparent cylinder placed under the phase mask where they mutually interfere and create interferograms forming dark and bright fringes parallel to the axis, particularly at the resist-coated wall of the cylinder of radius R. As a result of such a holistic exposure, a complete and uniform cylindrical latent grating of period $R\Lambda_\Phi/2$ and exactly $2N$ periods is formed in the photoresist layer if the $+$ and -1st orders only are considered. The transmitted 0th order does not interfere with any other diffraction order at the cylinder wall since it propagates along the cylinder axis without intersecting the cylinder wall. This means that the generally most difficult requirement to satisfy in phase-mask technology (the cancellation of the 0th order) is *a priori* satisfied. That the $+$ and -1st orders do form an interferogram and can print a latent grating at the resist-coated cylinder wall is not evident at first sight: in a first holistic exposure scheme [5], sketched in Fig. 1, right, the coaxial incident beam was first transformed by a cone into a conical wave with nonzero axial and radial k-vector components before impinging onto the radial phase mask. A large radial k-vector permits to project the radial phase-mask grating onto the cylinder wall quite close to the cylinder top with the inherent problem that the vertical direction of the 1st and 0th orders does not differ notably, which imposes an extinction of the 0th order to avoid the super-position of the double-period 0th/1st order onto the desired $+1$st/-1st grating. A damping of the 0th order efficiency under conical incidence is possible by adjusting the groove depth and line/space ratio in a high-index corrugated layer. However, this condition cannot be satisfied over a large range of periods: as the azimuthal period of the radial phase-mask grating varies proportionally with the radius, this condition on the cancellation of the 0th order finally results in a limitation of the length of the lines of the printable cylindrical grating.

The sketch on the right in Fig. 1 illustrates the fact that all three -1st, 0th, and $+1$st orders propagate with a nonzero radial component of their k-vector toward the cylinder wall. The $-$ and $+1$st orders intersect the latter and interfere there to form the desired latent grating [axial position a)], whereas they overlap with the damped 0th order further down the cylinder axis to form a weaker contrast interferogram of double period at axial position c).

In the present exposure scheme of essentially normal incidence (see Fig. 1, left), the only nonzero k-vector component of the diffracted orders is the azimuthal component. The interferogram created by the $+1$st/-1st orders diffracted by an elemental area of the phase-mask grating only

exists in the small overlap zone of the two orders under the considered elemental zone; it does not extend to the cylinder wall. Therefore, an interferogram is produced at the intersection of the considered +1st (−1st) order beam with the cylinder wall only if there is a corresponding elemental area of the phase mask at the same radius directing its −1st (+1st) order respectively to the same intersection. The annular geometry of the radial phase-mask grating and the circularly symmetrical polarization distribution of the circular incident beam imply that to each area of the radial grating at the radial abscissa r emitting a +1st diffraction order corresponds another area having the same radial abscissa and the same field emitting a −1st order intersecting the cylinder wall at the same intersection where these interfere. This representation of the interference at the cylinder wall by three discrete diffracted light beams emanating from three associated areas of the phase mask is only here to render the formation of an interferogram at the cylinder wall plausible and to show that, unlike in the configuration of [5] where the exposure can possibly be made by an azimuthal scan of the exposure beam, a uniform interferogram in the present new scheme can only be formed by a holistic exposure over 2π. As illustrated in the left-hand sketch, the intersection of the diffracted beams with the cylinder wall occurs further away at a larger axial distance from the phase mask, at position b). The exposure configuration gives rise to a global interference between the + and −1st order waves diffracted by the radial phase mask upon normal incidence of the circularly symmetrical beam. The azimuthal uniformity of the interferogram at the cylinder wall is ensured by the normally incident beam having a radial or an azimuthal polarization. The interferogram contrast does not depend on the diffraction efficiency of the + and −1st orders of the phase-mask grating since the 0th order does not intervene; therefore, the contrast does not depend on the incident beam being radially or azimuthally polarized. The interference contrast depends on the angle between the two electric field vectors of the interfering diffracted beams: the contrast is zero if this angle is 90°. Therefore, if the incident beam is radially polarized, the angle between the two associated areas in the phase-mask plane seen from the cylinder axis must not be close to 90°. If the incident beam is azimuthally polarized, the angle of the 1st order diffracted rays relative to the phase-mask plane must not be close to 45°.

3. The Geometry of the Phase-Mask Projection

The binary radial grating of the phase mask is defined at the surface of a fused quartz substrate. Its period $\Lambda_g(r) = r\Lambda_\Phi$ is proportional to the radius r within the annular grating zone $R_i < r < R_e$. The minimum period $\Lambda_g(R_i)$ is such that the + and −1st orders at least propagate in the transparent cylinder of refractive index n_s, i.e., $\Lambda_g(R_i) > \lambda/n_s$, where λ is the exposure wavelength, here the 442 nm line of a HeCd laser. There is no strict limit for the maximum period $\Lambda_g(R_e)$. It may be desired that there are no diffraction orders of order larger than 1 so as to prevent the formation of an interferogram of different spatial frequency at the cylinder wall that may overlap with the desired $\pm$1st order interferogram; in this case, the following condition applies: $\Lambda_g(R_e) < 2\lambda/n_s$. This risk is, however, limited since the higher diffraction orders m intersect the cylinder at a distance H_m from the phase-mask grating plane, which is notably smaller than H_1. H_m is given by

$$H_m(r) = \sqrt{R^2 - r^2} \cdot \sqrt{\left(\frac{n_s\Lambda_\varphi r}{m\lambda}\right)^2 - 1}. \tag{1}$$

The corrugation profile can be chosen rather freely since any interference with the 0th order is excluded. The main demand is on a sufficient diffraction efficiency of the 1st orders and, to a lesser extent, on a minimization of the 2nd orders if the second-order interferogram formed at a distance $H_2(r)$ has an overlap at the cylinder wall with the first-order interferogram. As shown in the cross section of Fig. 2, the phase-mask grating is in direct contact with the cylinder with index matching liquid in-between. For the diffraction efficiency to be large with a shallow corrugation, the latter was made in a high-index layer of PECVD Si_3N_4 of index close to 2- and 160-nm thickness. The structure parameters were derived from the specifications on a future shaft encoder.
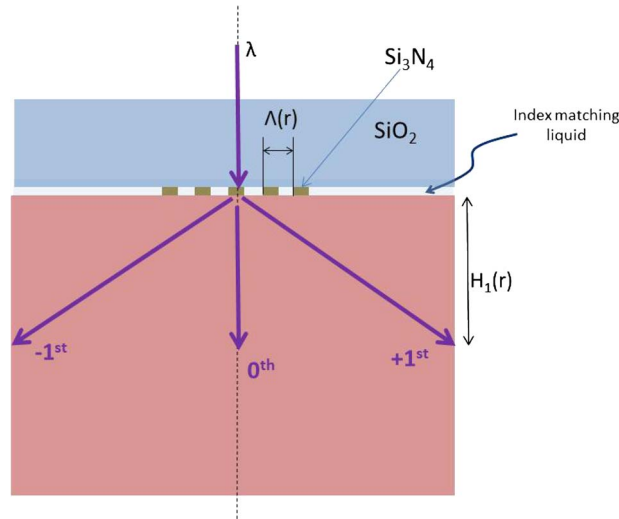
Fig. 2. Cross section of the diffraction event at an elemental area of the phase-mask grating in a plane parallel to the cylinder axis and normal to the radial lines at radius r.

A remarkable feature of the dependence of H_m on r is that it is not monotonic: there is a radius $r = r_{m\text{Max}}$ where H_m is maximum, $H_m = H_{m\text{Max}}$. This occurs at

$$r_{m\text{Max}} = R \cdot \sqrt{\frac{1 + \left(\frac{m\lambda}{n\lambda_\varphi R}\right)^2}{2}} \qquad (2)$$

and the maximum of H_m is

$$H_{m\text{Max}} = \frac{\left(\frac{n_s \Lambda_\varphi}{m\lambda}\right)^2 R^2 - 1}{\frac{2 n_s \Lambda_\varphi}{m\lambda}}. \qquad (3)$$

This implies that, if the center of the phase-mask grating ring is placed at $r = r_{1\text{Max}}$, i.e., if $(R_i + R_e)/2$ is substantially equal to $r_{1\text{Max}}$, the length of the cylindrical grating lines printed on the cylinder wall by the $+1$st and -1st order interferogram will be minimum. Therefore, if the aim is to obtain long cylindrical grating lines, the center of the phase-mask grating ring must be chosen where the derivative $dH_m(r)/dr$ is large. Advantage can be taken from the period magnification, which results from the cylindrical symmetry: by setting R large enough with respect to R_i and R_e, an interferogram period as large as desired can, in principle, be defined without any spurious over-modulation.

The future application example of the first cylindrical grating fabricated by the present phase-mask method is the submicrometer grating of a miniature holistic rotation encoder placed on the shaft of 8-mm diameter and having the integer number $2N = 2^{15}$ periods. The desired length of lines of the cylindrical grating lines is about 2–3 mm. The inner and outer radii R_i and R_e of the phase-mask radial grating are 1.2 and 2 mm. The number $N = 2^{14}$ of azimuthal periods defines an angular period $\Lambda_\Phi = 383.5$ μrad, which, in turn, defines the azimuthal periods $\Lambda_g(R_i) = 0.46$ μm and $\Lambda_g(R_e) = 0.776$ μm at radii R_i and R_e. This grating was e-beam written and etched by the University of Eastern Finland. With these data and the 442-nm exposure wavelength of a HeCd laser, the transmission through the phase mask is not single order: the second diffraction order does propagate as from the radius of 1.6 mm. However, the second-order interferogram forms at the cylinder wall notably closer to the phase mask than the first-order interferogram: using expression (1) for $H_1(R_i)$, which is the upper limit of the first-order interferogram, and for $H_2(R_e)$, which is the lower limit of the second-order interferogram, shows that there is no overlap between the
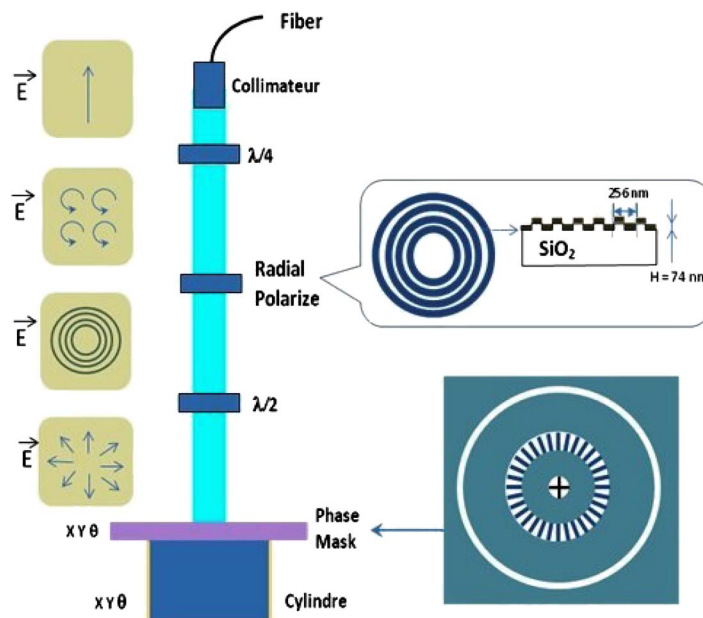
Fig. 3. Sketch of the exposure turret comprising a light delivery PM fiber, a half-wave plate, a polarizing waveguide grating, and the phase mask/cylinder assembly.

first- and second-order interferograms at the cylinder wall since $H_1(R_i) = 4.37$ mm and $H_2(R_e) = 2.7$ mm. As a matter of fact, the propagation of the 2nd orders in the cylinder does not represent the actual limit for a single spatial frequency interferogram at the cylinder wall since the phase-mask corrugation can easily be designed and fabricated to lead to a cancellation of the diffraction efficiency of the 2nd orders. The practical limit for a single order interferogram is, therefore, set by the cutoff of the 3rd order. It can, thus, generally be said that the maximum length of the printable grating is approximately given by $H_{1\text{Max}} - H_{3\text{Max}}$.

The exposure bench is a single-beam coaxial setup, as illustrated in Fig. 3. The linearly polarized beam of a HeCd laser at 442-nm wavelength is coupled into a polarization-maintaining fiber single mode at 442 nm. At the fiber end, it is collimated and circularly polarized. A radial polarizer based on resonant reflection from a circular line grating reflects the local TE polarization and transmits close to 100% of the local TM polarization [6]. The circular groove corrugation covers an area of 6-mm diameter; the radial period is 256 nm, which an e-beam only can write. The grating was written and also etched in fused silica by Fraunhofer IOF Jena. After the etching, a ZnS waveguide layer was deposited at a thickness of 60 nm selected to produce the resonant reflection of its fundamental TE_0 mode in the neighborhood of 442 nm.

4. The Technological Steps

Such a cylindrical diffractive element and the proposed method for its fabrication are completely outside the paradigm of planar microstructuring technologies inherited from microelectronics. The rationale of the cylindrical grating writing method is, thus, to define a highly accurate origination element that can be defined by planar technologies, then to project it into the warped 3-D space of the cylinder wall: the radial phase mask takes the best in precision and resolution of what e-beam writing can offer today with the most recent tools (Vistec EBPG 52000). Once the phase-mask projection parameters have been defined, all technological steps have to be adapted or reinvented: cylindrical substrate holding/handling, photoresist coating, alignment/centering procedures, exposure, and, last but not least, characterization. We report here on the preliminary laboratory process steps that have been developed to demonstrate the capability of the method to fabricate a cylindrical grating with an integer number of submicrometer periods in the photoresist coating at the cylinder wall.

Fig. 4. Absorptive film overcoating of the photoresist layer with vacuum holder.

The handling is all made by means of a dedicated silicone vacuum manipulator holding one of the polished ends of the transparent cylinder. The photoresist coating is made by controlled pulling under a constant vapor pressure. The photoresist is set in its linear or nonlinear regime depending on the desired grating profile, which can thus range between sinusoidal and binary. In the present fabricability demonstration, the positive photoresist Shipley 505 A is set outside its linear regime in order to get the easiest control of the corrugation geometry relative to the cylinder wall and to obtain the rectangular grooves needed by the future rotation sensor application [3]. The resist dip-coating process was calibrated initially by AFM on planar substrates with a targeted resist thickness of 400 nm. A very important aspect of the involved resist photochemistry is its possible compatibility with a PMMA cylindrical substrate. The reason is that the described method is not primarily aimed at cylindrical grating manufacturing but at obtaining a master that can then be replicated at very low cost by embossing or microinjection molding. The 3-D geometry of the element and the vulnerability of the microstructure at the element wall impose the master to be easily dissolvable chemically after a nickel shim has been grown. A complete chain of resist processes has been developed specifically on PMMA substrates to enable this mould technology for prismatic structures having a microstructure at the flank [7].

The photoresist coating at the cylinder wall is then coated by a light absorptive layer to first prevent the interferogram field from experiencing total internal reflection, secondly to prevent the formation of field nodes and antinodes in the resist layer. Fig. 4 illustrates the cylinder being held by the vacuum holder in the process step of absorptive layer coating.

The resist-coated cylinder is held in place against the phase-mask substrate with index matching liquid in-between by means of a gripper holding it in a zone of the wall where the grating will not be formed. High-resolution micropositioners permit to make the centering of the cylinder by visual inspection from the other polished cylinder end-face.

5. The Printed Grating

In order to compare the two exposure configurations represented in Fig. 1(a) and (b), the incident coaxial beam was expanded to a diameter larger than twice the outer radius of the phase-mask grating R_e. The cone of diameter smaller than $2R_i$ was centered and pasted. In so doing, the same incident beam is used to achieve the phase-mask projection according to both methods. The result is shown in the picture of Fig. 5, where a first cylindrical grating of about 1-mm groove length was printed close to the cylinder end by the cylindrical wave reflected by the cone, and a second grating deeper along the cylinder axis with groove length of more than 3 mm resulting from the direct diffraction of the normally incident beam. The aspect is very uniform and does not exhibit nonuniformity and stitching error. Simple optical microscope inspection reveals that both gratings have a single spatial frequency corresponding to that produced by the 1st orders of the phase-mask grating.
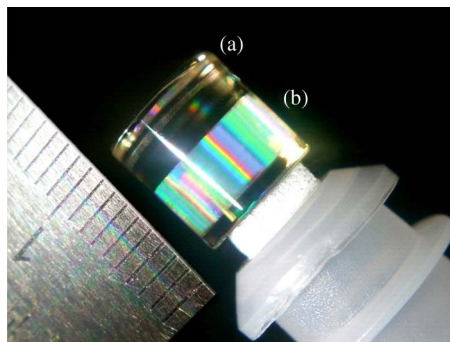
Fig. 5. Picture of two cylindrical gratings at the photoresist-coated wall. a) Printed under circularly symmetric conical incidence with a reflecting cone, b) printed by direct diffraction of the normally incident beam.
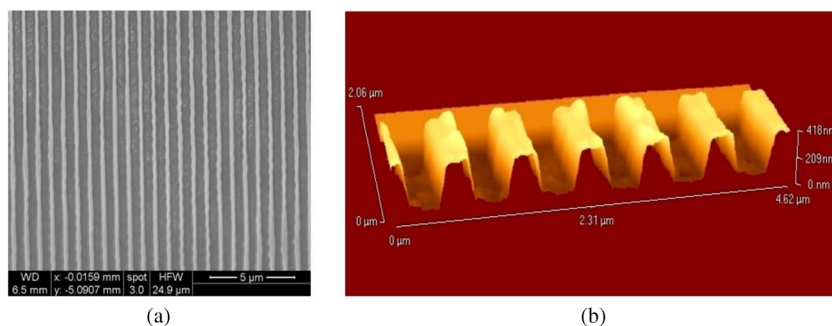

Fig. 6. Micromeasurement of the resist corrugation at the cylinder wall. a) SEM, b) AFM scan.

The characterization of the obtained resist corrugation is a problem in itself as the element cannot rest on a support without damaging the other side. The cylinder is held at both ends by a spring-loaded fixture in a U-shape support. Fig. 6(a) is the top SEM view of the photoresist grating at the cylinder wall, and Fig. 6(b) is the AFM scan of a few periods showing that the aspect ratio is larger than 1 and that there is no evidence of standing-wave (anti)nodes despite the relatively large groove depth due to the absorptive overcoating of the photoresist.

The corrugation is essentially binary with the groove bottom down to the cylinder surface, the line-top flat, a slight rounding of the top wedges, and slope of the resist walls close to vertical; the resist line height is close to the initial resist thickness of 400 nm, all this confirming that a corrugation of the type needed by an interferometric diffractive rotation sensor [3] is fabricable. No particular care was devoted at the present development stage to the uniformity of the light intensity distribution over the grating area. While a photoresist in its nonlinear regime is quite tolerant in this regard, as suggested by the remarkably uniform aspect of grating b) in Fig. 5, this will be an important concern in the printing of a sinusoidal grating profile for instance.

The SEM image reveals that the photoresist lines exhibit a small-amplitude high-spatial-frequency undulation. This is the result of a spurious interferogram created by the reflection of the diffracted order at the bottom of the cylinder, where no absorptive coating was used to permit the alignment between phase mask and cylinder.

6. Conclusion

A circularly symmetrical planar phase mask under the normal exposure of a circularly symmetrical beam creates at the wall of a cylinder a uniform interferogram having an integer number of dark and bright lines parallel to the cylinder axis. This extension of the applicability of phase-mask lithography to circularly symmetrical structures requires a more complex phase mask than in conventional

applications, but the transfer conditions are notably simplified since the problem of the 0th order cancellation is *a priori* solved. Not only can the described technique print subwavelength cylindrical gratings: advantage can be taken of the period magnification inherent to the properties of cylindrical waves to print large period gratings without the problem of having a multiharmonic interferogram.

Acknowledgment

References

[1] N. Trappe, R. Mahon, W. Ladigan, J. Murphy, and S. Withington, "The quasi-optical analysis of Bessel beams in the far infra-red," *Infrared Phys. Technol.*, vol. 46, no. 3, pp. 233–247, Jan. 2005.
[2] O. Parriaux, A. V. Tishchenko, and F. Pigeon, "Associating a lossless polarizing function in multilayer laser mirrors by means of a resonant grating," in *Proc. SPIE*, 2006, vol. 6187, pp. 72–79.
[3] O. Parriaux, Y. Jourlin, and N. Lyndin, "Cylindrical Grating Rotation Sensor," Eur. Patent EP2 233 892 A1, Sep. 29, 2010.
[4] K. Phan Huy, A. Morand, and P. Benech, "Modelization of the whispering gallery mode in microgear resonators using the Floquet–Bloch formalism," *IEEE J. Quantum Electron.*, vol. 41, no. 3, pp. 357–365, Mar. 2005.
[5] S. Tonchev, Y. Jourlin, C. Veillas, S. Reynaud, N. Lyndin, O. Parriaux, J. Laukkanen, and M. Kuittinen, "Subwavelength cylindrical grating by holistic phase-mask coordinate transform," *Opt. Exp.*, vol. 20, no. 7, pp. 7946–7953, Mar. 2012.
[6] G. A. Golubenko, A. S. Svakhin, V. A. Sychugov, and A. V. Tishchenko, "Total reflection of light from a corrugated surface of a dielectric waveguide," *Sov. J. Quantum Electron.*, vol. 15, no. 7, pp. 886–887, Jul. 1985.
[7] S. Tonchev, Y. Jourlin, S. Reynaud, M. Guttmann, M. Wissmann, R. Krajewski, and M. Joswik, "Photolithography of variable depth gratings on a polymer substrate for the mastering of 3D diffractive optical elements," in *Proc. 14th MOC*, Brussels, Belgium, Sep. 2008.